Clean Technologies and Environmental Policy (2022) 24:393–412
https://doi.org/10.1007/s10098-021-02235-4

ORIGINAL PAPER

Spatial optimization of photovoltaic-based hydrogen-electricity supply chain through an integrated geographical information system and mathematical modeling approach

Angel Xin Yee Mah[1,2] · Wai Shin Ho[1] · Mimi H. Hassim[3] · Haslenda Hashim[1] · Zarina Ab Muis[1] · Gabriel Hoh Teck Ling[4] · Chin Siong Ho[4]

Received: 5 January 2021 / Accepted: 31 October 2021 / Published online: 6 January 2022

Abstract

Hydrogen is a potential energy carrier for renewable energy as it has a clean emission when consumed. To implement hydrogen energy system in large-scale, a comprehensive hydrogen supply network should be built to supply the required hydrogen with optimal infrastructure arrangement. Although the optimization of hydrogen gas supply chain has been extensively studied, the investigation into an integrated hydrogen-electricity supply chain is still lacking. Considering the interconvertibility of hydrogen and electricity, this study presents a spatial optimization framework that integrates geographical information with mathematical modeling for the design and optimization of a photovoltaic-based hydrogen-electricity supply chain. The proposed framework allows the concurrent targeting of vehicle fuel and electricity demands as well as the identification of suitable locations for supply chain infrastructures. The case study results show that the minimum cost of hydrogen-electricity supply chain is about 14.9 billion USD/y assuming two days of autonomy, and the cost of battery constitutes 43% of the total supply chain cost. When the days of autonomy is 8 and above, hydrogen storage is preferred and electricity is regenerated from hydrogen using fuel cell.

✉ Wai Shin Ho
hwshin@utm.my

[1] Process Systems Engineering Centre (PROSPECT), Research Institute of Sustainable Environment (RISE), Universiti Teknologi Malaysia (UTM), 81310 Johor Bahru, Johor, Malaysia

[2] NUS Environmental Research Institute (NERI), National University of Singapore, Singapore 117411, Singapore

[3] Centre of Hydrogen Energy, Institute of Future Energy, Universiti Teknologi Malaysia (UTM), 81310 Johor Bahru, Johor, Malaysia

[4] UTM-Low Carbon Asia Research Centre, Program of Urban and Regional Planning, Faculty of Built Environment and Surveying, Universiti Teknologi Malaysia (UTM), 81310 Johor Bahru, Johor, Malaysia

Graphical abstract

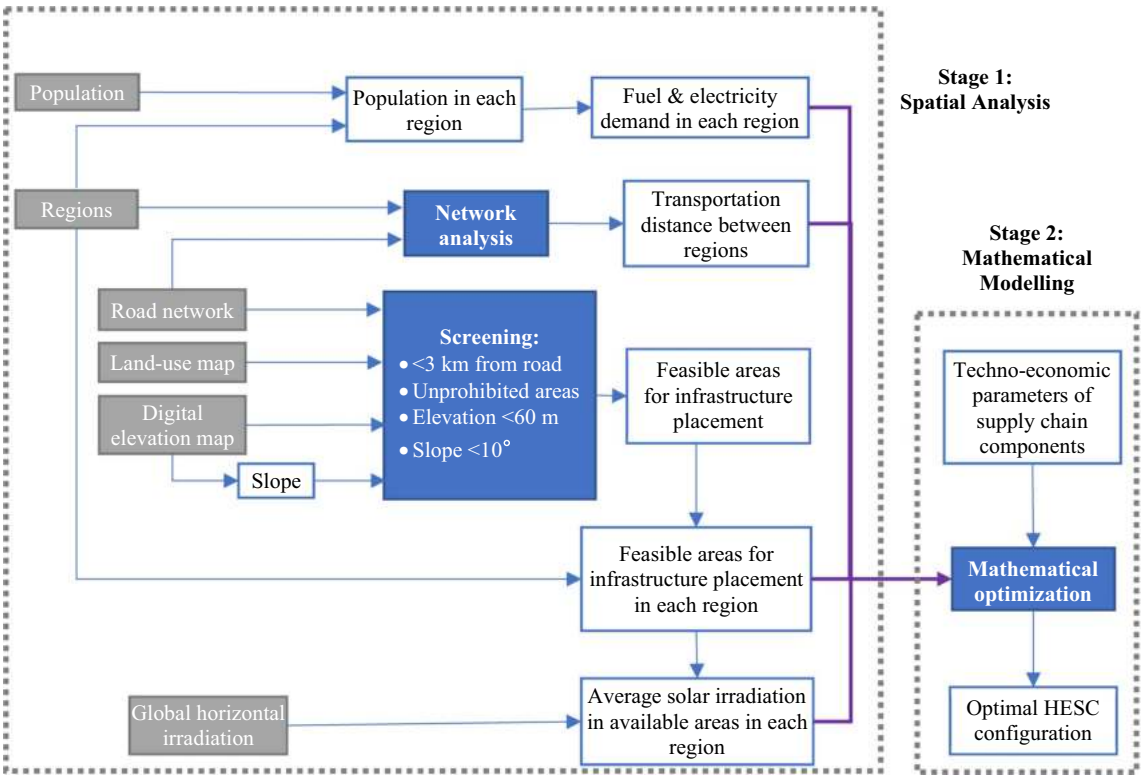

Keywords Hydrogen supply chain · GIS · MILP · Spatial analysis · Hydrogen energy system

List of symbols

Sets

c	Set of hydrogen in different storage and transportation forms
j	Set of study regions
k	Set of study regions, identical to set j

Parameters

$A_j^{Feasible}$	Feasible area for the placement of supply chain facilities at region j, m^2
$AAKT$	Annual average distance travelled by vehicle, km
B_c^{FC}	Binary defining the form of hydrogen c that can be used for fuel cell
B_c^{RF}	Binary defining the form of hydrogen c that can be used in refueling station
B_c^{Pipe}	Binary defining the form of hydrogen c that can be transported with pipeline
$B_{j,k}^{Trans}$	Binary defining whether the product can be transported from region j to region k
B_c^{Truck}	Binary defining the form of hydrogen c that can be transported with trailer
BS^{Eff}	Battery storage efficiency
$C^{unitcapex}$	Unit capital cost of equipment, USD/unit
$C^{unitopex}$	Unit operating cost of equipment, USD/unit/y
$C^{unitrep}$	Unit replacement cost of equipment, USD/unit
$CONV^{Eff}$	Converter efficiency
CRF	Capital recovery factor
$D^{Autonomy}$	Days of autonomy
E_j^{Demand}	Electricity demand in region j, kWh/d
E^{losses}	Electricity losses during transmission and distribution
$ED^{percapita}$	Electricity demand per capita, kWh
EL^{Eff}	Electrolyzer efficiency
$Elec^{cost}$	Electricity cost, USD/kWh
f^{Land}	Land use factor based on the area of solar panel
FC^{Eff}	Fuel cell efficiency
FCV^{FE}	Fuel economy of fuel cell vehicle, kg/km
H_j^{Demand}	Hydrogen demand in region j, kg/d
H^E	Hydrogen energy content, kWh/kg
i	Interest rate
M	A dimensionless large number for the definition of binaries in MILP model

P^{rate} Supply chain penetration rate
$Petrol^{cost}$ Petrol cost, USD/L
Pop_j Population in region j
Pop^{Total} Total population in all study regions
PRV^{FE} Fuel economy of petrol vehicle, L/km
PR_c^{Losses} Hydrogen losses when being processed to convert into form c
PV^{Eff} Solar panel efficiency
RF_c^{Losses} Losses of hydrogen form c during unloading and handling at refueling station
SR_j Solar irradiation at region j, kWh/m^2/d
VH^{Total} Total number of vehicles in study regions
Y^{CL} Lifespan of supply chain component, y
Y^{SL} Lifespan of supply chain, y

Binary variables

$B_j^{EImport}$ Binary variable defining whether electricity is imported to region j
$B_j^{EHImport}$ Binary variable defining whether electricity imported to region j is used to produce hydrogen
B_j^{EProd} Binary variable defining whether electricity is produced in region j
$B_j^{HImport}$ Binary variable defining whether hydrogen is imported to region j
B_j^{HProd} Binary variable defining whether hydrogen is produced in region j

Continuous variables

A_j^{PV} Area of solar panel at region j, m^2
C^{acapex} Annualized capital cost of equipment, USD/y
C^{arep} Annualized replacement cost of equipment, USD/y
C^{opex} Annual operating cost of equipment, USD/y
$Cost^{Extra}$ Extra cost incurred to conventional fuel and electricity, USD/y
E^{Cap} Equipment capacity
E_j^{FC} Electricity produced by fuel cell in region j, kWh/d
E_j^{G} Electricity generated by solar PV in region j, kWh/d
E_j^{Import} Electricity imported to region j, kWh/d
$E_j^{ImporttoE}$ Electricity imported to region j used for electricity demand, kWh/d
$E_j^{ImporttoH}$ Electricity imported to region j used for hydrogen demand, kWh/d
$E_j^{toDemand}$ PV electricity produced in region j used to satisfy the local electricity demand, kWh/d
E_j^{toE} PV electricity produced in region j utilized in the form of electricity, kWh/d
$E_{j,k}^{toExport}$ PV electricity produced in region j exported to region k, kWh/d
E_j^{toH} PV electricity produced in region j used to synthesize hydrogen, kWh/d
E_j^{S} Energy stored in battery, kWh
H_j^{G} Hydrogen generation at region j, kg/d
$H_j^{EImport}$ Hydrogen produced from imported electricity at region j, kg/d
$H_{j,c}^{Export}$ Hydrogen in form c to be exported from region j to other regions, kg/d
$H_{j,c}^{FC}$ Hydrogen reacted in fuel cell in form c in region j, kg/d
$H_{j,c}^{Import}$ Hydrogen in form c to be imported to region j, kg/d
$H_{j,k,c}^{P}$ Hydrogen transported using pipeline in form c from region j to region k, kg/d
$H_{j,c}^{Pin.EIH}$ Hydrogen produced using electricity imported to region j and to be converted into form c, kg/d
$H_{j,c}^{Pin,LC}$ Hydrogen produced using local electricity in region j and to be converted into form c, kg/d
$H_{j,c}^{Pout,EIH}$ Hydrogen produced using electricity imported to region j converted into form c, kg/d
$H_{j,c}^{Pout,LC}$ Hydrogen produced using local electricity in region j converted into form c, kg/d
$H_{j,c}^{RF}$ Hydrogen received at refueling station in form c in region j, kg/d
$H_{j,c}^{S}$ Amount of hydrogen stored in form c in region j, kg/d
$H_{j,c}^{toSelf}$ Hydrogen in form c to be used within region j, kg/d
$H_{j,k,c}^{T}$ Hydrogen transported using truck in form c from region j to region k, kg/d
PV_j^{Cap} Capacity of solar panel at region j, kWp
TCC Annualized capital cost of supply chain, USD/y
TOC Annual operating cost of supply chain, USD/y
$TotalCost^{Con}$ Total cost of conventional energy use in a year, USD/y
$TotalCost^{HSC}$ Total cost of supply chain in a year, USD/y
TRC Annualized replacement cost of supply chain, USD/y

Introduction

Hydrogen energy can play a major role in addressing energy transition issues as it is able to provide high-density energy storage and flexible capacities. It is a versatile fuel that can be synthesized from various energy sources such as renewables and fossil fuels. In addition, hydrogen can be stored in large quantities for long periods and the stored energy can be released through combustion or electrochemical conversion (Martin et al. 2020). It also has a high heating value and clean emission (Acar and Dincer 2018).

As hydrogen only emits water at the point of use, synthesizing hydrogen from renewable energy sources would make the entire energy system clean and sustainable. While most of the global hydrogen production was derived from fossil fuel, IEA (2019) reported that the declining costs of solar PV and wind electricity have generated interest in electrolytic hydrogen, and can be seen in several demonstration projects in recent years. Hydrogen is deemed to be able to decarbonize global energy through various applications such as an alternative fuel for automobiles or temporary energy storage for renewables (Hydrogen Council 2017). Excess electricity produced from renewables can be converted to hydrogen via electrolysis of water, and the produced hydrogen will be able to serve as backup for an energy system.

Before hydrogen can be applied in the energy sector, it has to be produced and processed from raw materials. A typical hydrogen supply chain (HSC) consists of energy sources, production technologies, storage and transportation, as well as the final utilization point of hydrogen energy. The optimization of HSC is crucial to ensure smooth product logistics and a balanced supply–demand ratio with minimum investment cost.

Past studies on hydrogen supply chain optimization

Optimization method is the most popular choice for the design and modeling of HSC to determine the best configuration that fulfils the predefined economic, safety, or environmental criteria (Dagdougui 2012). As mathematical optimization allows for the modeling of complex HSC that is subject to a series of design variables (Maryam 2017), many studies have employed it for the optimization of hydrogen supply chain. As shown in Table 1, many recent studies have employed mixed-integer linear programming (MILP) model for HSC optimization with cost as the objective function. The hydrogen product is normally stored as compressed gas (GH_2) or in cryogenic liquid form (LH_2) to be utilized as vehicle fuel.

GIS-integrated mathematical optimization of hydrogen supply chain

Unlike mathematical optimization models, a geographic information system (GIS)-based approach is not generic but dependent on the spatial conditions at a national or regional scale to include factors such as transportation network, land use, and population. According to Dagdougui (2012), both optimization and GIS-based approaches have their strengths and weakness: optimization model allows for complex modeling of HSC but the spatial conditions are neglected,

Table 1 Mathematical optimization studies on hydrogen supply chain

Year	Model	Objective function	Hydrogen form (storage period)	Hydrogen application	Refs.
2016	MILP	Minimize cost	LH_2 (15 days)	Vehicle fuel	Kim and Kim (2016)
2016	MILP	Minimize cost	LH_2 (10 days)	Vehicle fuel	Woo et al. (2016)
2017	MILP	Minimize cost	GH_2	Vehicle fuel	Won et al. (2017)
2017	MILP	Minimize cost	GH_2, LH_2 (0.15 days)	Vehicle fuel	Moreno-Benito et al. (2017)
2018	MILP	Maximize net present value, minimize GHG emission	GH_2	Vehicle fuel	Ogumerem et al. (2018)
2018	MILP	Minimize cost	GH_2, LH_2	Vehicle fuel	Ochoa Bique and Zondervan (2018)
2019	MILP	Maximize net present value	LH_2	Vehicle fuel	Cho and Kim (2019)
2020	Genetic algorithm	Minimize cost, CO_2 emission and risk	LH_2 (3 days)	Vehicle fuel	Robles et al. (2020)
2020	MILP	Minimize cost	GH_2, LH_2 (3 days)	Vehicle fuel	Seo et al. (2020)
2020	MILP	Minimize cost	GH_2, LH_2	Vehicle fuel	Li et al. (2020)
2021	MILP	Minimize cost	GH_2	Vehicle fuel	Shamsi et al. (2021)

while a GIS-based model considers the spatial conditions but is only applicable for simple problems. Therefore, an integrated mathematical optimization and GIS model can complement the strengths of both methods.

In the past, there have been several studies that coupled GIS with mathematical optimization model. Johnson and Ogden (2012) used GIS to develop a hydrogen demand model which is based on population data, fuel cell vehicle efficiency, average distance travelled, and the per capita vehicle ownership. The candidate pipeline network is defined following the existing pipeline. Almaraz et al. (2015) employed GIS to locate the existing hydrogen infrastructure and computed the delivery distance using the road network. The results obtained in mathematical optimization (selected energy sources, production and storage capacities, refueling stations) will be displayed on a map using ArcGIS. Samsatli et al. (2016) developed an energy network model known as STeMES to optimize the design and operation of integrated wind-hydrogen-electricity networks for decarbonizing the domestic transport sector of Great Britain. The land availability for onshore wind turbine siting is decided by geographical factors such as wind speed, slope of land, accessibility to road network, connectivity to national grid, protected areas, as well as distance to human activities and wildlife. Welder et al. (2018) conducted a spatial–temporal optimization of a future energy system in Germany for power-to-hydrogen application in their transportation and industrial sector. The land available for onshore wind turbine placement is assessed by eliminating water bodies and also by setting up buffer zones around water bodies, residential areas, commercial areas, industrial areas, and critical infrastructures such as power lines, major roads, and railways. In addition, land that is far from road networks, protected land, and the region with low wind speed are excluded during the land eligibility analysis. The new pipeline routes are then recommended to be built along high-pressure compressed natural gas, highway, or railway routes.

Samsatli and Samsatli (2019) developed a spatial–temporal Value Web Model that can simultaneously determine the design and operation of hydrogen-to-heat value chains based on wind power. The spatial distribution and temporal variation of the heat demands in Great Britain are considered during the optimization. Meanwhile, site suitability analysis is performed to identify the available area for construction in each zone. The spatial information on UK Exclusive Economic Zone, shipping routes, and water depth are used to screen the suitable areas for offshore wind turbine placement. Welder et al. (2019) assessed the hydrogen reconversion pathways to transport the surplus electricity from northern Germany to southern Germany. The surplus electricity can be delivered to the demand region through grid expansion or pipeline transportation of hydrogen. The latter requires the conversion of surplus electricity into hydrogen prior to pipeline transportation, and reconversion back to electricity when hydrogen reaches the demand site. The economic feasibility of reconversion technologies such as gas turbines combined cycle power plants, gas engines, or fuel cells has been investigated. The suitable routes for hydrogen pipeline are determined according to the existing high-pressure natural gas grid, motorways, and railway tracks. Meanwhile, the hydrogen sources with surplus electricity generation are recommended to be close to the starting point of new power cables. Reuß et al. (2019) evaluated various technologies for hydrogen storage and transportation on a nationwide scale for Germany energy system in 2050. Locations with excess electricity production are determined as hydrogen sources, while the fuelling stations are defined as hydrogen sinks. The truck routing model is developed with an average truck speed of 60 km/h on highways and 30 km/h on all other roads. The hydrogen pipeline system is designed by performing candidate grid development, topology selection, mass flow determination and diameter selection using the existing high-pressure natural gas grid as the potential routes. The fueling station locations are clustered using k-means clustering to determine the hub position for hydrogen transmission and distribution.

Summary of literature review

Through literature review, several research gaps have been identified:

i. The lack of integration of hydrogen supply chain with other energy supply chains such as heat and electricity. As hydrogen supply system is not standalone, its integration with other supply chains is an important research direction, and the critical factor for such integration is to identify the appropriate "insertion points" through which the supply chains are connected (Li et al. 2019). Based on the review in Table 1, many recent studies have targeted hydrogen production for vehicle fuelling. In Sect. 2.1, which reviews the GIS-integrated mathematical optimization models, Welder et al. (2018) investigated the optimal energy system with hydrogen application in transportation and industry; Samsatli and Samsatli (2019) studied the hydrogen-to-heat value chains, while Welder et al. (2019) employed hydrogen as energy storage to transport electricity from surplus region to deficit region. Nevertheless, the optimization of an integrated hydrogen-electricity network fulfilling both hydrogen and electricity demands has yet to be investigated.
ii. As reviewed in Table 1, most hydrogen supply chain studies only consider conventional hydrogen storage and transportation methods (GH_2 or LH_2) but not other possible options such as liquid organic hydrogen

carrier (LOHC). In Sect. 2.1, Reuß et al. (2017, 2019) evaluated the use of LOHC over conventional options but the scope of energy system began with hydrogen production in electrolyzer where the residual loads are used as the energy source. However, this would underestimate the levelized cost of hydrogen as the cost of electricity production is not considered.

iii. Most hydrogen supply chain studies only consider fixed days of autonomy/storage holding period but the effect of increasing and decreasing the storage period has not been evaluated. For instance, Kim and Kim (2016), Woo et al. (2016), Moreno-Benito et al. (2017), Robles et al. (2020), Seo et al. (2020) had considered certain periods of hydrogen storage to be used as backup supply. However, the assumptions vary between studies (ranges from 0.15 to 15 days) and the influence of such decisions were not evaluated. In addition, considering the interconvertibility of hydrogen and electricity, as well as the suitability of hydrogen as long-term energy storage, the effect of storage period would be more obvious in an integrated hydrogen-electricity network as described in (i).

To address the identified research gaps, this study aims to develop a comprehensive framework for the spatial optimization of PV-based hydrogen-electricity supply chain (HESC). In the proposed framework, site suitability analysis in Malaysia is conducted using GIS to determine feasible areas for the placement of supply chain components. The optimal siting and capacities of supply chain infrastructures for concurrent targeting of vehicle fuelling and electricity demands are then determined through a mathematical optimization model. In mathematical modeling, the storage and transportation of hydrogen in the form of compressed gas, cryogenic liquid, or LOHC will be considered. Moreover, the influence of days of autonomy assumptions on the optimal modes of production, storage and transportation of hydrogen and electricity is investigated.

Methodology

In this study, a optimization framework comprising of GIS and mathematical modeling is proposed for the optimization of HESC that caters for vehicle fuelling and electricity demands. Figure 1 shows the superstructure of the HESC

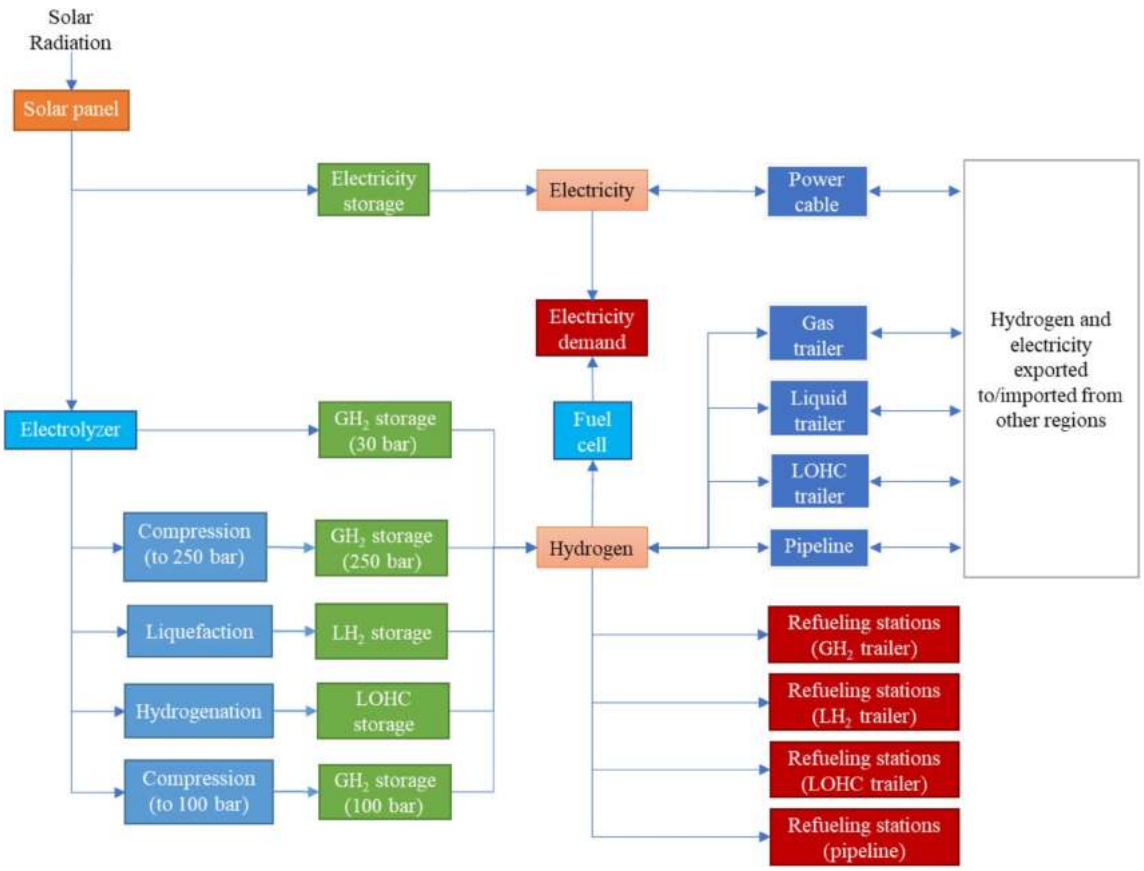

Fig. 1 Superstructure of PV-based hydrogen-electricity production system

which involves electricity production from solar radiation through PV systems. The electricity produced can be exported to other regions via power cables or converted into hydrogen via electrolyzer. Hydrogen produced can be stored in gaseous form (GH_2), liquid form (LH_2), or bonded with LOHC upon processing and transported to other regions through trucks or pipelines. There are four types of refueling stations based on the mode of hydrogen transportation; namely in the form of GH_2 trailer, LH_2 trailer, LOHC trailer, or pipeline. The electricity demand of a region can be fulfilled by PV electricity, imported electricity, or electricity produced from hydrogen. Hydrogen reacts with oxygen in a fuel cell to produce electricity. Meanwhile, the hydrogen demands in refueling stations are satisfied by the hydrogen produced from PV electricity or imported electricity.

Figure 2 illustrates the workflow of the proposed framework which comprises a two-stage approach for the spatial optimization of HESC. In the first stage, GIS is employed for spatial data processing and site suitability analysis. Spatial information such as land use, road network, elevation, and slope are used to determine the potential areas for infrastructure placement. Meanwhile, spatial population data is used to estimate regional vehicle fuelling and electricity demands. The transportation distance between study regions will be determined using network analysis tool in ArcGIS. Second stage of the framework involves the formulation of a mathematical optimization model to identify the optimal HESC configuration for targeted fuelling and electricity demands.

Spatial analysis

Figure 3 shows the districts in Johor, Malaysia which are used as study regions for the spatial optimization of HESC in this work. The most populated locations in each of the districts have been indicated on the map. These are useful when determining the transportation distance between districts.

To identify feasible areas for the placement of supply chain infrastructures, several geographical constraints will be used for the screening process. Figure 4a–e display the spatial factors considered while also including solar irradiation, population, land elevation, transportation network, and land use data. The global horizontal irradiation data is obtained from Solargis (2020), population data from WorldPop (2018), digital elevation of the land from USGS (2015), road data from DIVA-GIS (2021), and the land use map from MaCGDI (2010).

Based on the population data, the potential electricity and hydrogen fuel demands in each region can be estimated through Eqs. (1) and (2), and the required parameters are given in Table 2.

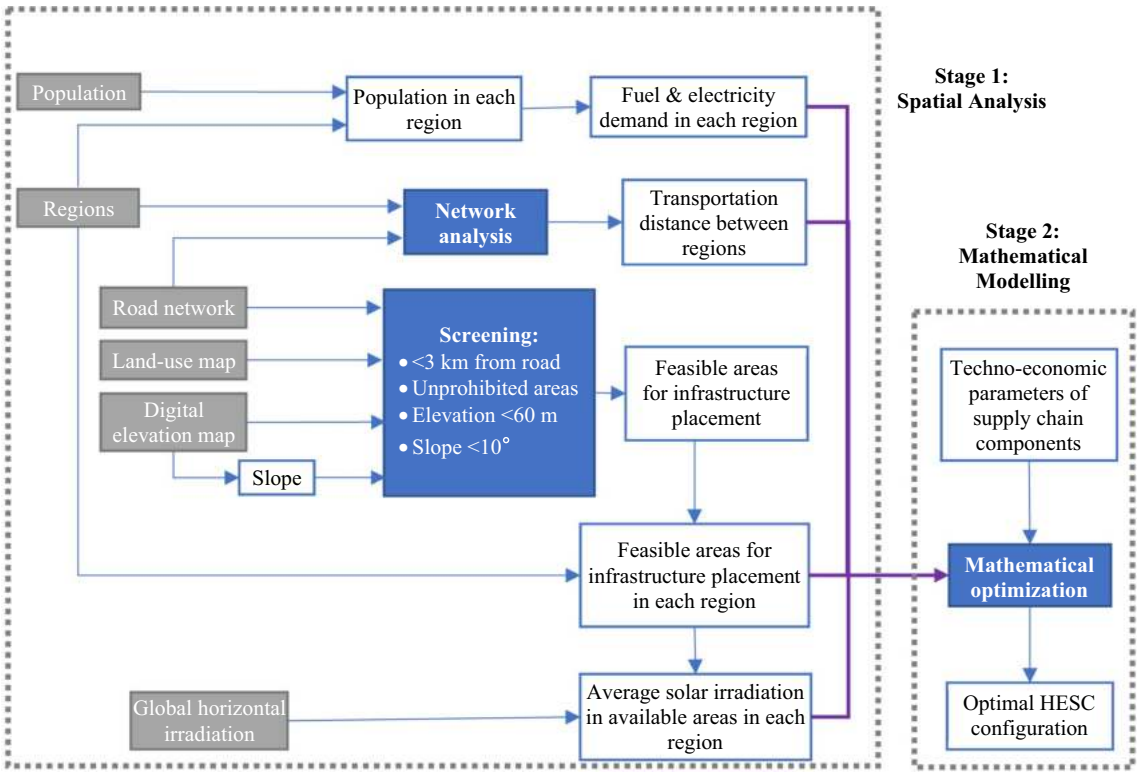

Fig. 2 Generic workflow of proposed framework

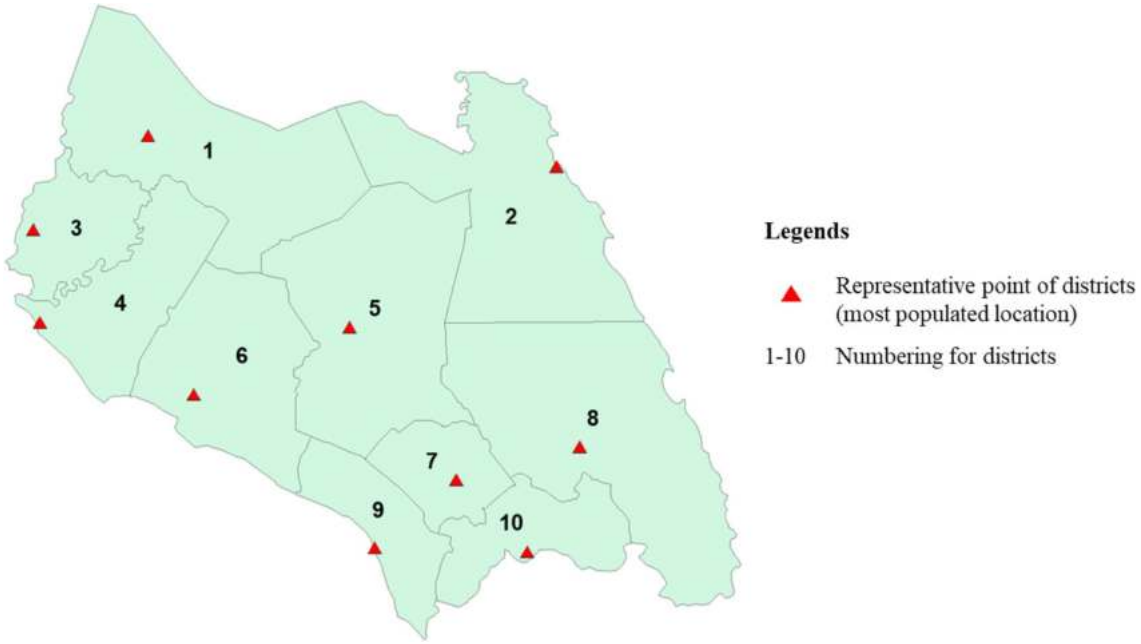

Fig. 3 Johor Districts

$$H_j^{\text{Demand}} = \frac{\text{Pop}_j}{\text{Pop}^{\text{Total}}} \times VH^{\text{Total}} \times \frac{AAKT}{365} \times FCV^{FE} \quad \forall j \tag{1}$$

$$E_j^{\text{Demand}} = Pop_j \times \frac{ED^{\text{percapita}}}{365} \quad \forall j \tag{2}$$

The spatial analysis is performed using ArcMap 10.5. As shown in Fig. 5a–d, the feasible areas for supply chain infrastructure placement, average solar irradiation, fuel and electricity demands in all regions can be determined through spatial analysis. Based on Fig. 5, region 4 receives the highest solar irradiation while region 10 has the highest fuel and electricity demands. Table 3 displays the transportation distance between the regions. With the processed spatial data, an optimization model is used to determine the optimal arrangement of supply chain infrastructures to fulfil regional energy demands using electricity produced from solar PV.

Mathematical model

Mathematical optimization is used to determine the least-cost HESC network. This section describes mathematical equations for the objective function, mass and energy balance, as well as the generic costing of equipment. As the costing of specific supply chain components is lengthy and dependent on the techno-economic parameters provided, the detailed calculations are not displayed here but in the Supplementary Material.

Objective function

The objective function of this model is to minimize the cost of hydrogen-electricity supply chain, which is given by the summation of total capital, operating, and replacement costs of the supply chain components in a year:

$$\text{TotalCost}^{HSC} = TCC + TOC + TRC \tag{3}$$

The generic formulas for the annualized capital and replacement costs of equipment are extracted from Huang et al. (2019). Equation (4) shows the calculation for annualized capital cost, where the capital recovery factor is given by Eq. (5). Meanwhile, the annualized replacement cost can be calculated using Eq. (6). The annual operating cost of equipment is given by Eq. (7).

$$C^{\text{acapex}} = E^{\text{Cap}} C^{\text{unitcapex}} CRF \tag{4}$$

$$CRF = \frac{i(i+1)^{YSL}}{(i+1)^{YSL} - 1} \tag{5}$$

$$C^{\text{arep}} = E^{\text{Cap}} C^{\text{unitrep}} \frac{i}{(i+1)^{YCL} - 1} \tag{6}$$

$$C^{\text{opex}} = E^{\text{Cap}} C^{\text{unitopex}} \tag{7}$$

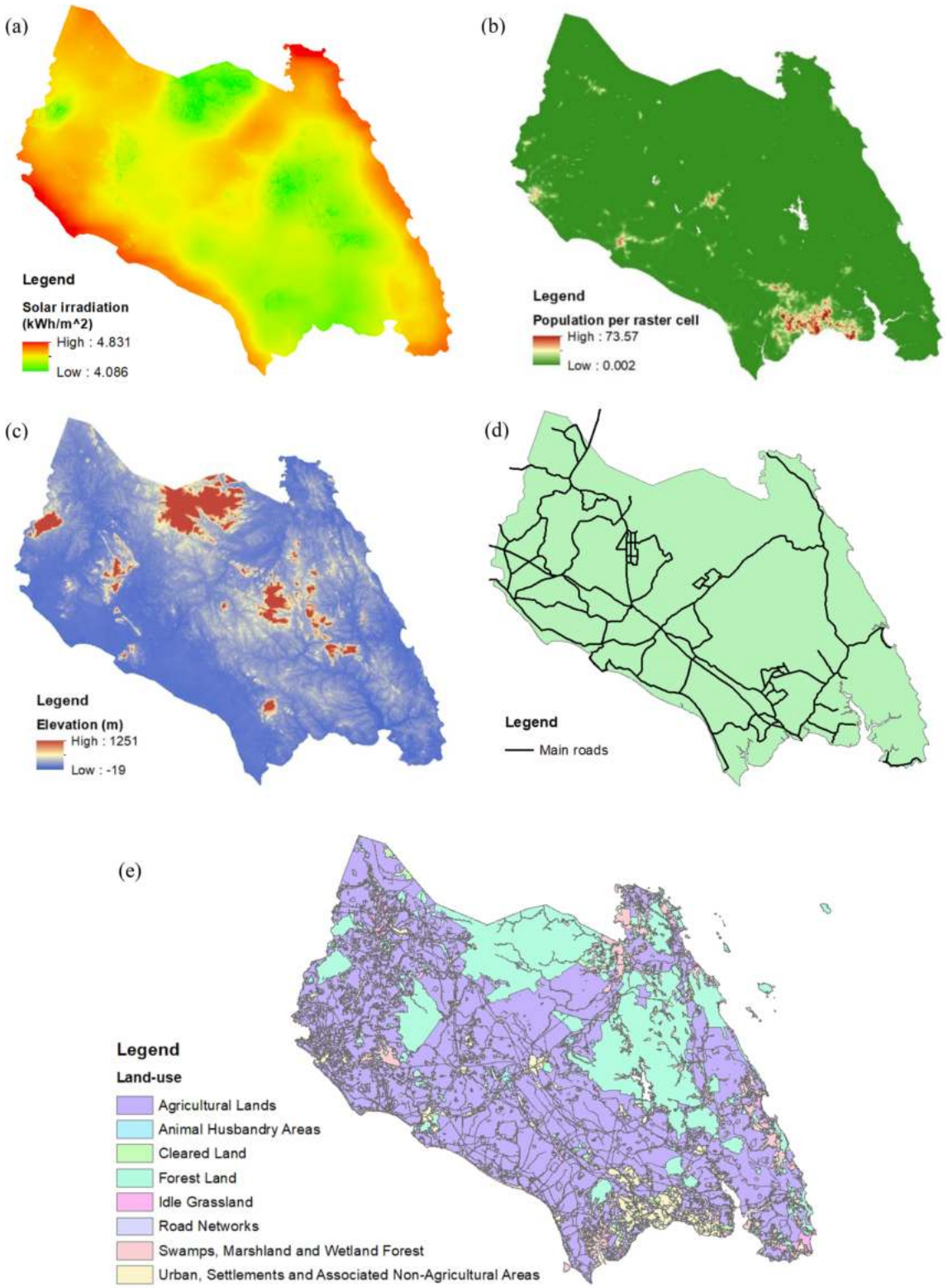

Fig. 4 Geographical considerations for the construction of processing site (**a**) solar irradiation (**b**) population (**c**) elevation (**d**) road network (**e**) land use

Table 2 Electricity and fuel consumption information in Johor

Parameter	Value	Unit	Refs.
Total number of cars in Johor[a]	1,884,735		Shabadin et al. (2014)
Total distance travelled in a year	16,342.30	km/y	Shabadin et al. (2014)
Fuel economy of fuel cell electric vehicle	0.0076	kg/km	H2 Mobility (2021)
Electricity consumption per capita	4553	kWh/y	Energy Commission (2019)

[a]Extracted from (Shabadin et al. 2014) and projected to year 2020 assuming 5% annual vehicle growth rate

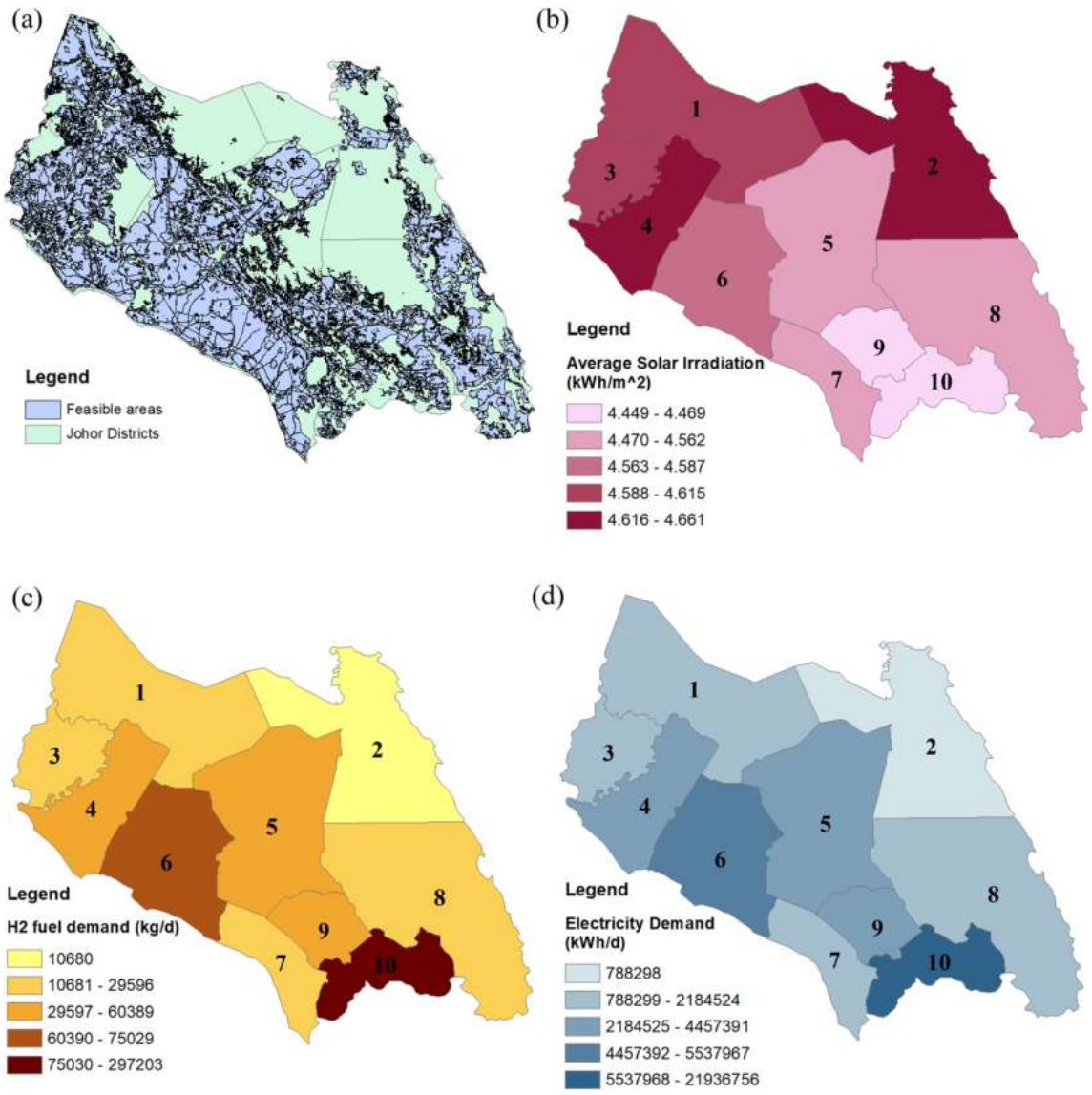

Fig. 5 Spatial analysis results (**a**) feasible areas for infrastructure placement (**b**) average daily global horizontal irradiation (**c**) hydrogen fuel demand (**d**) electricity demand

Electricity generation, storage and transmission

Equation (8) computes the electricity generation from solar radiation. The peak power of solar panel can be determined using Eq. (9), while Eq. (10) bounds the land-use to be within the available area in a region. The constant f^{Land} is used to scale the land use of the entire system based on the area occupied by solar panels.

Table 3 Transportation distance between the study regions (km)

Region	Region									
	1	2	3	4	5	6	7	8	9	10
1	0	205	52	79	109	96	145	189	149	171
2	205	0	205	198	96	149	130	88	174	120
3	52	205	0	27	109	77	145	189	150	171
4	79	198	27	0	102	52	139	183	143	165
5	109	96	109	102	0	53	70	114	78	100
6	96	149	77	52	53	0	89	133	93	115
7	145	130	145	139	70	89	0	44	54	31
8	189	88	189	183	114	133	44	0	88	35
9	149	174	150	143	78	93	54	88	0	53
10	171	120	171	165	100	115	31	35	53	0

$$E_j^G = SR_j A_j^{PV} PV^{Eff} \quad \forall j \tag{8}$$

$$PV_j^{\text{Cap}} = A_j^{PV} PV^{Eff} \quad \forall j \tag{9}$$

$$A_j^{PV} f^{\text{Land}} \le A_j^{\text{Feasible}} \quad \forall j \tag{10}$$

Equation (11) indicates that the electricity produced in solar panel can be utilized in the form of electricity or converted into hydrogen. The electricity available is either used to fulfil the electrical demand or exported to other regions, as indicated in Eq. (12). Considering the mismatch between electricity production and demand, the efficiency losses in energy storage, BS^{Eff} is taken into account. Equation (13) shows the net amount of electricity delivered to each region. The electricity imported by a region can be used for electricity or hydrogen demands as defined in Eq. (14).

$$E_j^G = E_j^{toE} + E_j^{toH} \quad \forall j \tag{11}$$

$$E_j^{toE} BS^{Eff} CONV^{Eff} = E_j^{\text{toDemand}} + \sum_k E_{j,k}^{\text{toExport}} \quad \forall j \tag{12}$$

$$E_j^{\text{Import}} = \sum_k E_{k,j}^{\text{toExport}} \left(1 - E^{\text{losses}}\right) \quad \forall j \tag{13}$$

$$E_j^{\text{Import}} = E_j^{\text{ImporttoE}} + E_j^{\text{ImporttoH}} \quad \forall j \tag{14}$$

Equation (15) defines that the electricity demand of a region must be satisfied by the sum of imported electricity, locally produced PV electricity, and the electricity produced from hydrogen in fuel cell. Note that the electricity produced in fuel cell should be converted to alternating current (AC) from direct current (DC) as the electrical load typically requires AC to function. The electricity produced in fuel cell is given by Eq. (16) where the binary B_c^{FC} defines the form of hydrogen that can be used in fuel cell.

$$E_j^{\text{ImporttoE}} + E_j^{\text{toDemand}} + E_j^{FC} \text{CONV}^{eff} \ge E_j^{\text{Demand}} \quad \forall j \tag{15}$$

$$E_j^{FC} = \sum_c H_{j,c}^{FC} B_c^{FC} H^E FC^{Eff} \quad \forall j \tag{16}$$

Equation (17) specifies that a region should not be producing and importing electricity at the same time, and the respective binaries can be defined using Eqs. (18) and (19). M represents a constant with large value to allow the binary definition. Taking Eq. (18) as an example, when E_j^{toE} is positive, the term $\frac{E_j^{toE}}{M}$ is greater than 0 but less than 1, and the binary B_j^{EProd} must be 1 for the expression to be valid. The same concept applies for the definition of binary $B_j^{EImport}$.

$$B_j^{E\text{Prod}} + B_j^{E\text{Import}} \le 1 \quad \forall j \tag{17}$$

$$B_j^{E\text{Prod}} \ge \frac{E_j^{toE}}{M} \quad \forall j \tag{18}$$

$$B_j^{E\text{Import}} \ge \frac{E_j^{\text{Import}}}{M} \quad \forall j \tag{19}$$

For this study, the electricity storage requirement is estimated based on the 'days of autonomy' concept. The energy storage will be installed at the electricity-producing site as shown in Eq. (20).

$$E_j^S \ge E_j^{toE} D^{\text{Autonomy}} \quad \forall j \tag{20}$$

Hydrogen production, storage, and transportation

The amount of hydrogen produced using locally generated electricity can be computed using Eq. (21). On the other hand, the electricity imported from other regions can also be used to produce hydrogen as illustrated in Eq. (22).

Note that the imported electricity has to be converted from AC into DC before inputting into an electrolyzer.

$$H_j^G = \frac{E_j^{toH} EL^{Eff}}{H^E} \quad \forall j \tag{21}$$

$$H_j^{E\text{Import}} = \frac{E_j^{\text{Import to}H} \text{CONV}^{Eff} EL^{Eff}}{H^E} \quad \forall j \tag{22}$$

Hydrogen can be stored in several forms such as compressed gas, cryogenic liquid, or liquid organic hydrogen carrier. Thus, the hydrogen produced in electrolyzer has to be converted into suitable forms prior to storage. Equation (23) defines the sum of locally produced hydrogen to be converted to other forms. Considering the losses when converting hydrogen from one form to another, Eq. (24) gives the net amount of hydrogen remaining upon conversion. The same applies to the hydrogen produced from imported electricity, as shown in Eqs. (25) and (26).

$$H_j^G = \sum_c H_{j,c}^{\text{Pin},LC} \quad \forall j \tag{23}$$

$$H_{j,c}^{\text{Pout},LC} = H_{j,c}^{\text{Pin},LC}(1 - PR_c^{\text{Losses}}) \quad \forall j, c \tag{24}$$

$$H_j^{E\text{Import}} = \sum_c H_{j,c}^{\text{Pin}.EIH} \quad \forall j \tag{25}$$

$$H_{j,c}^{\text{Pout},EIH} = H_{j,c}^{\text{Pin},EIH}(1 - PR_c^{\text{Losses}}) \quad \forall j, c \tag{26}$$

Equation (27) shows that the processed hydrogen can either be utilized locally or transported to other regions. Equation (28) represents the mass balance of hydrogen available in a region, where the binaries are used to define the form of hydrogen that can be transported to refueling stations or used on-site for electricity generation in fuel cells. The sum of hydrogen transported to refueling stations should satisfy the hydrogen fuel demand in each region as defined in Eq. (29) where the loss of hydrogen during unloading or handling at refueling station is taken into account.

$$H_{j,c}^{\text{Pout},LC} + H_{j,c}^{\text{Pout},EIH} = H_{j,c}^{\text{toSelf}} + H_{j,c}^{\text{Export}} \quad \forall j, c \tag{27}$$

$$H_{j,c}^{\text{toSelf}} + H_{j,c}^{\text{Import}} = H_{j,c}^{RF} B_c^{RF} + H_{j,c}^{FC} B_c^{FC} \quad \forall j, c \tag{28}$$

$$\sum_c H_{j,c}^{RF}(1 - RF_c^{\text{Losses}}) \geq H_j^{\text{Demand}} \quad \forall j \tag{29}$$

Equations (30) and (31) restrict a region from producing and importing hydrogen at the same time, while the binaries B_j^{HProd}, $B_j^{HImport}$, and $B_j^{EHImport}$ can be defined using Eqs. (32), (33), and (34).

$$B_j^{H\text{Prod}} + B_j^{H\text{Import}} \leq 1 \quad \forall j \tag{30}$$

$$B_j^{H\text{Prod}} + B_j^{EH\text{Import}} \leq 1 \quad \forall j \tag{31}$$

$$B_j^{H\text{Prod}} \geq \frac{E_j^{toH}}{M} \quad \forall j \tag{32}$$

$$B_j^{H\text{Import}} \geq \frac{\sum_c H_{j,c}^{\text{Import}}}{M} \quad \forall j \tag{33}$$

$$B_j^{EH\text{Import}} \geq \frac{E_j^{\text{Import to}H}}{M} \quad \forall j \tag{34}$$

Equation (35) constrains the total hydrogen inventory to be equal to or greater than the required backup supply.

$$H_{j,c}^S \geq H_{j,c}^{\text{Pout},LC} D^{\text{Autonomy}} \quad \forall j, c \tag{35}$$

Hydrogen can be transported from one region to another using truck or pipeline. Equations (36) and (37) define the amount of hydrogen exported from/imported to a region respectively. The binaries B_c^{Truck} and B_c^{Pipe} define which form of hydrogen can be transported using truck or pipeline, while $B_{j,k}^{Trans}$ defines whether the product can be transported from region j to region k.

$$H_{j,c}^{\text{Export}} = \sum_k H_{j,k,c}^T B_c^{\text{Truck}} B_{j,k}^{\text{Trans}} + \sum_k H_{j,k,c}^P B_c^{\text{Pipe}} B_{j,k}^{\text{Trans}} \quad \forall j, c \tag{36}$$

$$H_{j,c}^{\text{Import}} = \sum_k H_{k,j,c}^T B_c^{\text{Truck}} B_{j,k}^{\text{Trans}} + \sum_k H_{k,j,c}^P B_c^{\text{Pipe}} B_{j,k}^{\text{Trans}} \quad \forall j, c \tag{37}$$

Optimal HESC network

The optimization model is configured for various case studies to evaluate the economic performance of the proposed HESC network under different considerations to include the following:

- Base case scenario to determine the baseline cost of the proposed HESC network.
- Optimal cost and configuration of HESC with reduced/increased days of autonomy to identify the impact of energy storage requirement on the supply chain.

- Optimal cost of HESC when subjected to various electricity and hydrogen fuel penetration rates to determine suitable product charges.

The mixed-integer linear programming (MILP) model is formulated in GAMS and solved using CPLEX solver. The software is deployed on a HP Elitebook 850 G5 with Intel Core i5-8250U (1.60 GHz) processor and 8 GB RAM. The time required to obtain a solution is about 52 min and the model statistics are listed in Table 4.

Base case

Through mathematical optimization, the minimum cost of HESC for the base case scenario is determined to be 14.9 billion USD/y. Based on the cost breakdown displayed in Fig. 6, battery constitutes the highest proportion of cost followed by solar panel, electrolyzer, and converter. Figure 7a and b show the location of supply chain components and the product transportation network. In Fig. 7a, it can be observed that solar panels and battery systems are required in all regions. Nevertheless, only regions 1, 2, 4, and 9 require electrolyzers. This indicates that although all regions are producing electricity from solar PVs, only a few regions use PV electricity to produce hydrogen. According to Fig. 7b, hydrogen is transported from regions 2 and 4 to other regions, which also indicates that the hydrogen produced in regions 1 and 9 is only used for local demand. As most of the hydrogen is transported using GH_2 trailers, most regions have refueling stations to receive hydrogen from GH_2 trailers. Meanwhile, hydrogen is transported from region 4 to 10 through pipelines. This is likely due to the high transportation load and long transportation distance that makes pipeline transportation more feasible than truck transportation. Overall, it is found that hydrogen is mainly produced in regions with high solar irradiation and transported to other regions. Table 5 displays the capacities of major equipment in each region, and region 4 has the highest solar panel capacity.

While the base scenario considers two days of autonomy which allows the energy storage to supply two days worth of loads without any support from generation sources, the cost of optimal HESC network with fewer and more days of autonomy is inspected in next section. On the other hand, the suitable fuel and electricity charges for the HESC network to be cost-competitive in comparison to conventional energy system will also be discussed in the following section.

Table 4 Model Statistics

Blocks of Equations	112
Blocks of Variables	107
Single Equations	13,194
Single Variables	13,386
Discrete Variables	6,530
Resource Usage	3097.375 s

Influence of days of autonomy toward optimal HESC configuration

Days of autonomy represent the number of days an energy storage can supply the loads without energy generation. For this study, days of autonomy means the number of no-sun days that an energy storage can support. Figure 8 shows the optimal cost of HESC subjected to various days of

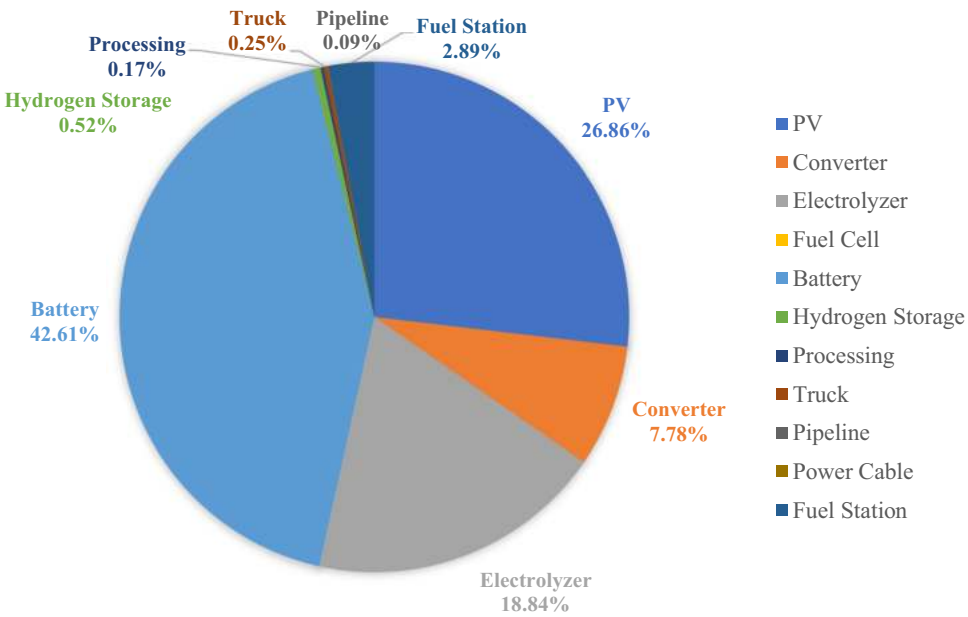

Fig. 6 Cost breakdown of optimal HESC network

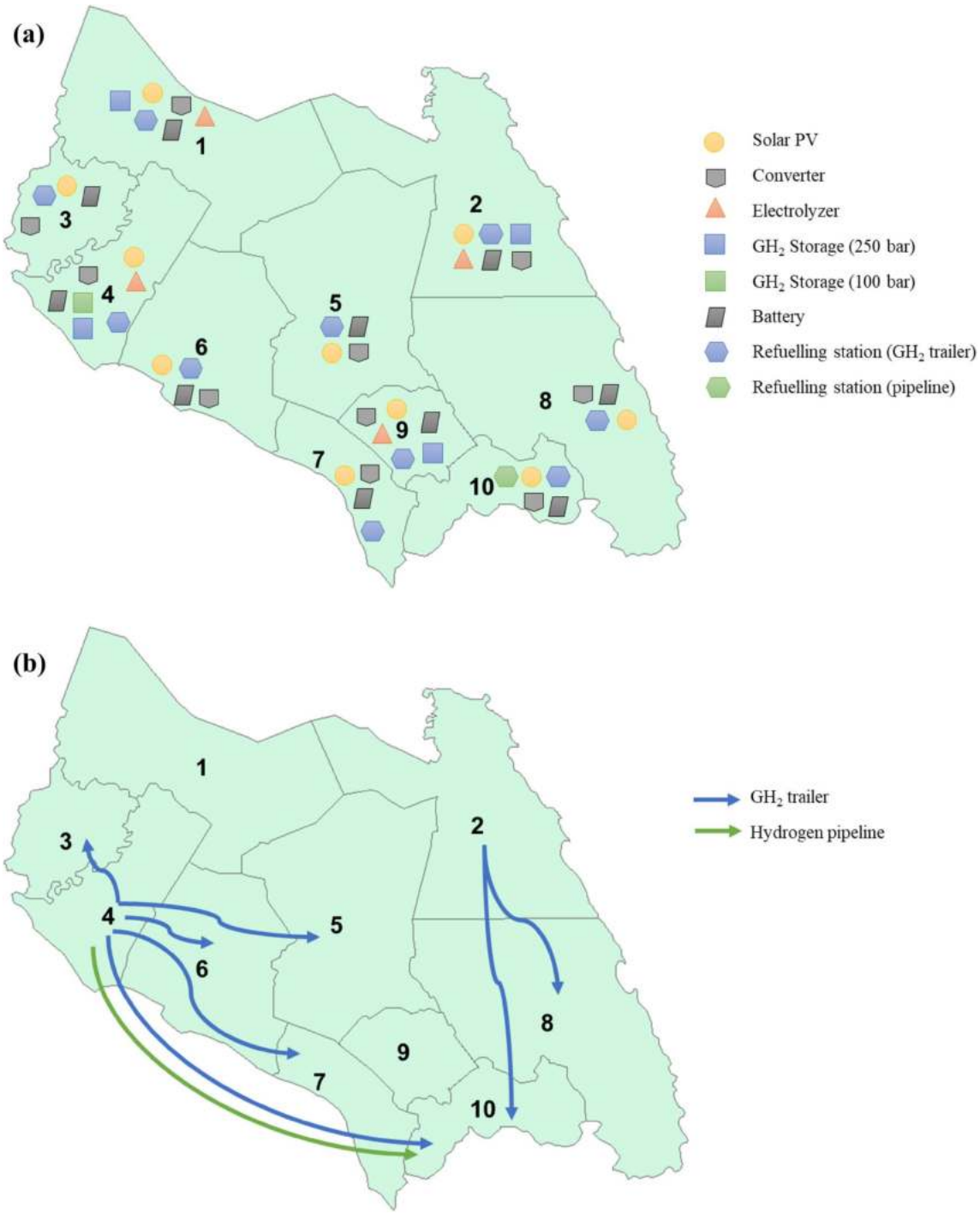

Fig. 7 Optimal HESC network: (**a**) infrastructure placement (**b**) transportation network

autonomy. Overall, the HESC cost increases with the days of autonomy. As the days of autonomy increases from 5 to 8, a significant cost reduction is observed for batteries and converters, while the total cost of solar panel, electrolyzer, fuel cell, and hydrogen storage have increased sharply. This indicates that more electricity is regenerated from hydrogen, and hydrogen storage is preferred as the days of autonomy increases. Based on Fig. 9, it is observed that the battery system is no longer employed when the days of autonomy is 8 or above. This is accompanied by a sharp rise in GH_2 storage requirements for pipeline transportation. In addition, LOHC storage is employed when the days of autonomy is 5 or above. Figure 10 presents the proportion of hydrogen storage with different days of autonomy. With 1 or 2 autonomy

Table 5 Capacities of main equipment (base case scenario)

Region	Solar panel capacity (MWp)	Converter capacity (MW)	Electrolyzer capacity (MW)	Battery capacity (MWh)	Hydrogen Storage (tonnes)	
					GH_2 (250 bar)	GH_2 (100 bar)
1	921	588	333	6763	59	0
2	1125	210	915	2441	165	0
3	400	400	0	4618	0	0
4	6495	878	5617	10,236	517	499.8
5	1032	1032	0	11,773	0	0
6	1495	1495	0	17,145	0	0
7	1235	1235	0	13,800	0	0
8	568	568	0	6465	0	0
9	743	474	268	5400	48	0
10	6106	6106	0	67,916	0	0

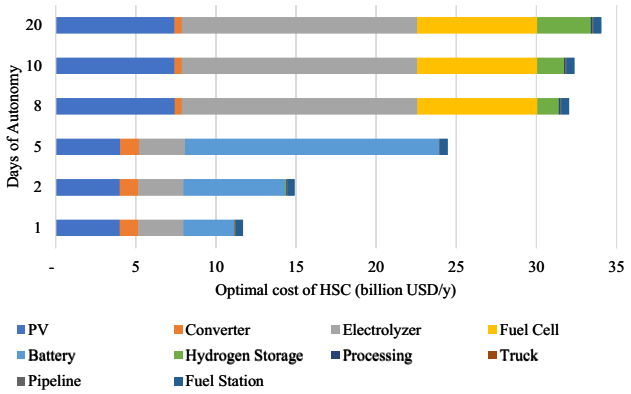

Fig. 8 Optimal cost of HESC with various days of autonomy

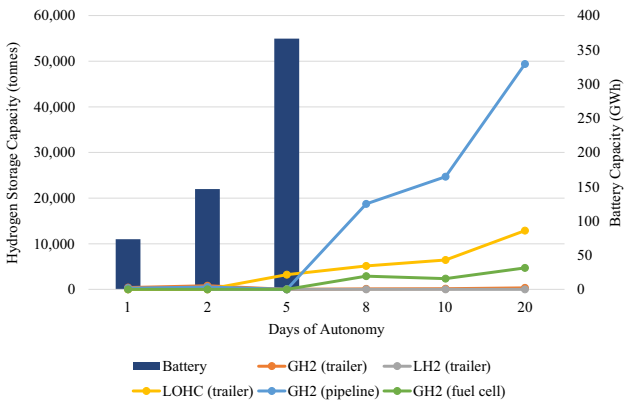

Fig. 9 Capacities of hydrogen and battery storage with various days of autonomy

days, the hydrogen is mainly stored in gaseous form to be transported via pipelines and trailers. Meanwhile, LOHC storage is preferred when the days of autonomy is set to 5.

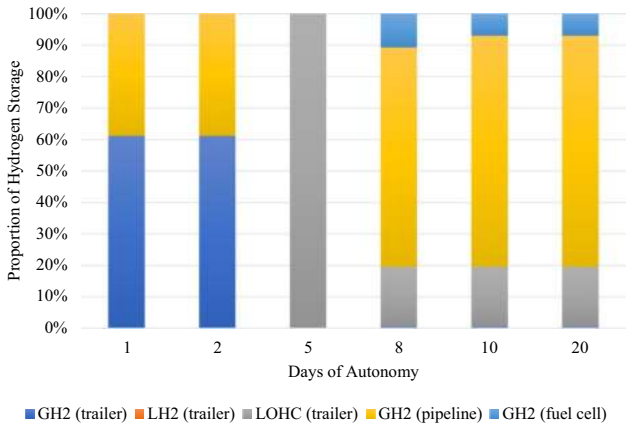

Fig. 10 Proportion of hydrogen storage with various days of autonomy

When the days of autonomy is 8 and beyond, the gaseous storage for pipeline and fuel cell becomes significant.

Figure 11 displays the optimal infrastructure placement and transportation network of the HESC when 8 days of autonomy is targeted. By comparing Figs. 11 and 7 (base case), Fig. 11 has fewer regions with solar panel installation but more regions with fuel cell, LOHC-based storage, transportation and refueling stations. There are no regions with battery system. In Fig. 11a, all regions are equipped with fuel cell systems instead of battery systems. PV systems and electrolyzers are only required in regions 1, 2, and 4. According to Fig. 11b, hydrogen is transported from regions 2 and 4 to other regions through GH_2 trailers, LOHC trailers, or hydrogen pipelines. Nevertheless, only LOHC-based refueling stations are required in all regions. This implies that hydrogen transported via GH_2 trailers and pipelines are not used for vehicle fuelling. By connecting this to the findings in Fig. 9 where the hydrogen storage at 100 bar (for pipeline transportation) increases rapidly when the battery system is

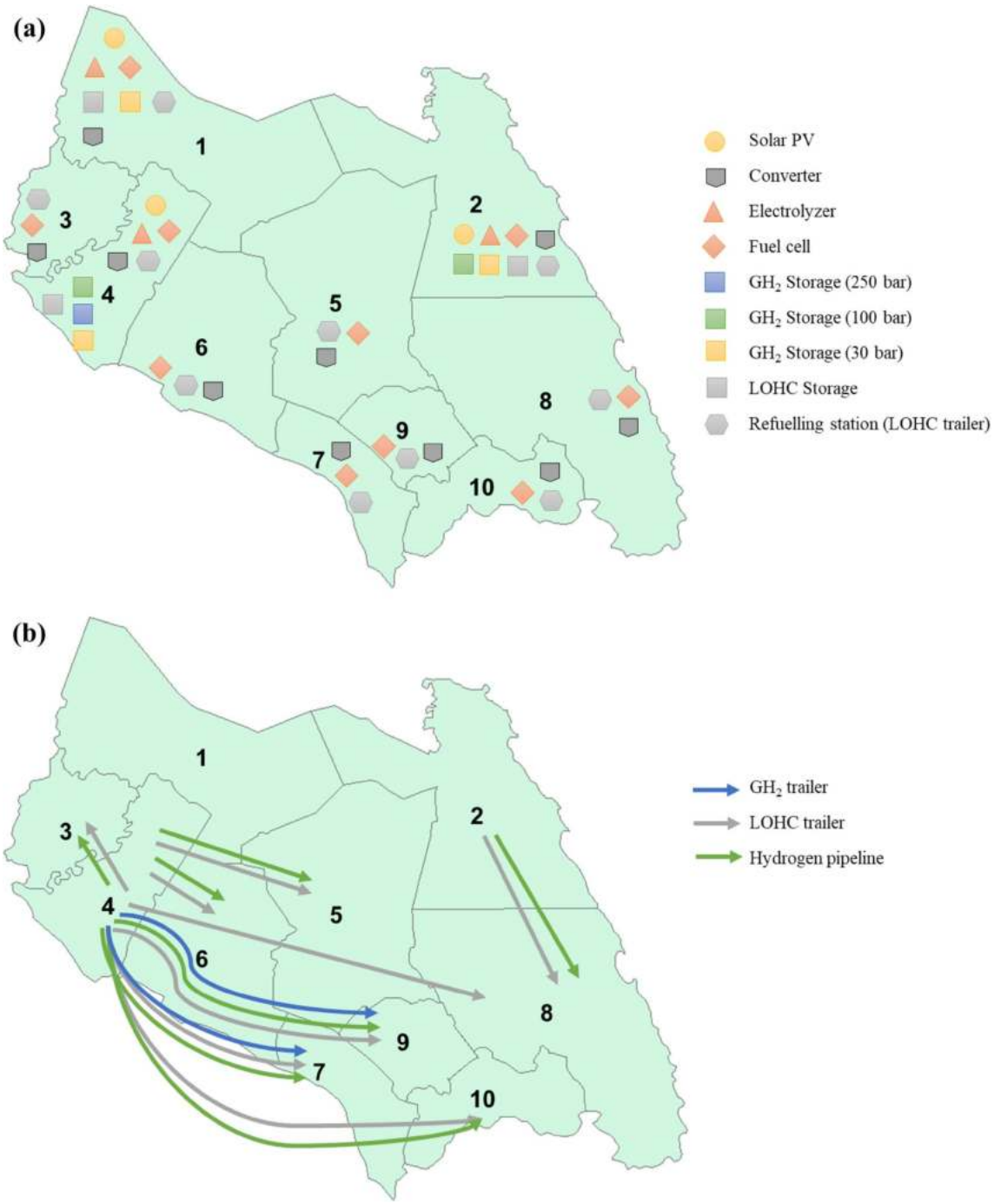

Fig. 11 Optimal HESC network (8 days of autonomy): (**a**) infrastructure placement (**b**) transportation network

unused, it can be deduced that the hydrogen transported in gaseous form is used for electricity production in fuel cell.

Cost-competitiveness of HESC network

Despite the high cost of HESC network, sensitivity analysis is conducted to identify the suitable charges for vehicle fuel and electricity for the proposed HESC network to be cost-competitive. Equation (38) is used to compute the total cost of conventional energy use based on the fuel and electricity demands defined in this study.

$$\text{TotalCost}^{\text{Con}} = \left(\frac{\sum_j H_j^{\text{Demand}}}{FCV^{FE}} PRV^{FE} \text{Petrol}^{\text{cost}} + \sum_j E_j^{\text{Demand}} \text{Elec}^{\text{cost}} \right) \times 365 \tag{38}$$

According to IEA (2019), the cost of producing hydrogen from renewable electricity could fall 30% by 2030 due to the declining costs of renewables and the upscaling of hydrogen production when the fuel cells and electrolyzers can benefit from mass manufacturing. On the other hand, the cost reduction benefit from large-scale production of solar PVs might have plateaued, but there is significant room to scale further in the manufacturing of batteries (IEA 2020). Thus, two scenarios are evaluated for the sensitivity analysis:

- *Scenario 1* The costs of supply chain infrastructures remain the same as in the base case scenario.
- *Scenario 2* The cost of battery is reduced by 50%, and the costs of electrolyzer and fuel cell are 70% of their initial values. Meanwhile, the costs of other supply chain infrastructures remain the same as in the base case scenario

For this sensitivity analysis, the cost of electricity will be expressed in USD/kWh, and the cost of fuel will be expressed in liter gasoline-equivalent, USD/L. The costs of fossil-based petrol and electricity are raised at the same rate until the total cost of conventional energy use, $TotalCost^{Con}$ is the same as the cost of the proposed HESC network, $TotalCost^{HSC}$.

Figure 12 shows the result of sensitivity analysis and it can be observed that the costs of petrol and electricity need to elevate by about 500% in scenario 1 for the green HESC network to be cost-competitive. This means that the fuel cost should be at least 3 USD/L and the electricity cost should be 0.36 USD/kWh. For scenario 2, about 300% increment in the original petrol and electricity costs will be required. This corresponds to a fuel cost of 2 USD/L and an electricity cost of 0.24 USD/kWh.

Considering the cases where green HESC network does not fulfil 100% of the energy demand, non-renewable energy sources (mainly from fossil fuel) will still be used to make up the difference. As demonstrated in Eq. (39), a 10% penetration rate of HESC network will require 90% of the energy demand be produced using conventional energy system. Increasing the tariff of conventional energy to higher rates will result in extra income from petrol and electricity sales, as shown in Eqs. (40) and (41). The extra income can be used to subsidize the green HESC network to reduce its investment cost as displayed in Eq. (42). The fuel and electricity

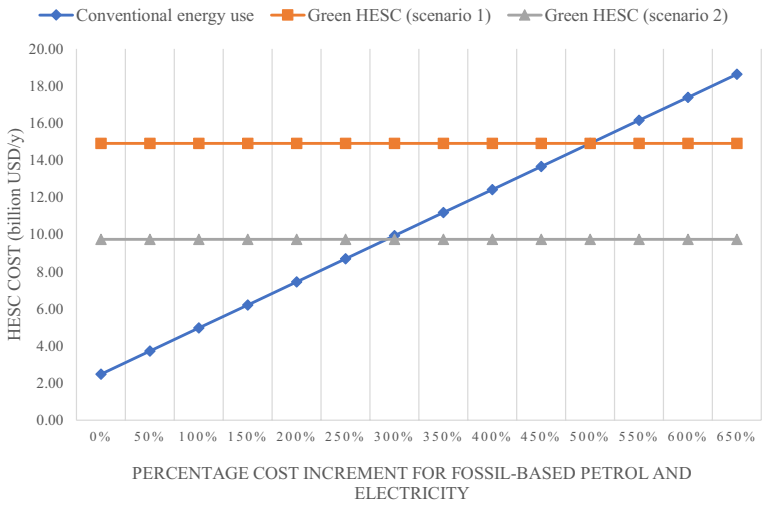

Fig. 12 Cost of energy use when subjected to various fossil-based petrol and electricity charges

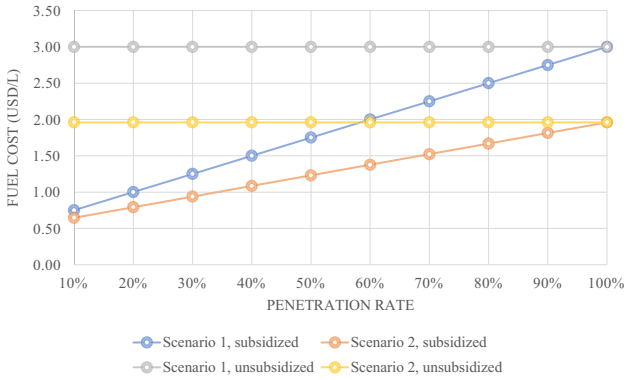

Fig. 13 Required fuel cost at various penetration rates of HESC network

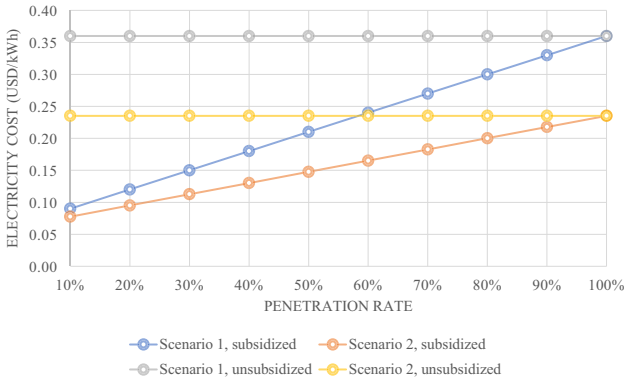

Fig. 14 Required electricity cost at various penetration rates of HESC network

costs are iterated until the cost of conventional energy, $TotalCost^{Con,new}$ equals the cost of the subsidized HESC network, $TotalCost^{HSC,new}$.

$$\mathrm{TotalCost}^{\mathrm{Con}} = \left[\left(\frac{\sum_j H_j^{Demand}}{FCV^{FE}} PRV^{FE} \mathrm{Petrol}^{\mathrm{cost}} + \sum_j E_j^{\mathrm{Demand}} \mathrm{Elec}^{\mathrm{cost}}\right) \times 365\right]\left(1 - P^{\mathrm{rate}}\right) \tag{39}$$

$$\mathrm{TotalCost}^{\mathrm{Con,new}} = \left[\left(\frac{\sum_j H_j^{\mathrm{Demand}}}{FCV^{FE}} PRV^{FE} \mathrm{Petrol}^{\mathrm{cost,new}} + \sum_j E_j^{\mathrm{Demand}} \mathrm{Elec}^{\mathrm{cost,new}}\right) \times 365\right]\left(1 - P^{\mathrm{rate}}\right) \tag{40}$$

$$\mathrm{Cost}^{\mathrm{Extra}} = \mathrm{TotalCost}^{\mathrm{Con,new}} - \mathrm{TotalCost}^{\mathrm{Con}} \tag{41}$$

$$\mathrm{TotalCost}^{\mathrm{HSC,new}} = \mathrm{TotalCost}^{\mathrm{HSC}} - \mathrm{Cost}^{\mathrm{Extra}} \tag{42}$$

Figures 13 and 14 display the required fuel and electricity costs with various penetration rates of HESC network. Overall, with the extra income from petrol and electricity sales used to subsidize the HESC network, the required costs are significantly lower than the unsubsidized scenario. At 100% penetration level, both the subsidized and unsubsidized scenarios have the same outcome as the conventional energy is no longer used, and there is no additional income to subsidize the HESC network. From Figs. 13 and 14, it can be observed that when the HESC network is subsidized, the required costs of fuel and electricity are similar for scenarios 1 and 2 when the penetration rate is low. Nevertheless, as the penetration rate increases, the difference between scenarios 1 and 2 becomes more significant.

Conclusion

This study presents an integrated GIS and mathematical optimization framework for the spatial optimization of hydrogen-electricity supply network. Through this study, four research gaps have been addressed: (i) the integration of hydrogen and electricity supply network in a single HESC optimization model, (ii) site suitability analysis using GIS to determine suitable areas for the installation of supply chain infrastructures, (iii) the storage and transportation of hydrogen in the form of LOHC has been considered in addition to the conventional gaseous and liquefied hydrogen storage, (iv) the impact of days of autonomy to the optimal supply chain configuration.

The proposed methodology has been demonstrated through a case study in Johor, Malaysia. Results showed that the least-cost HESC network in base case scenario would require an investment of 14.9 billion USD/y. By assuming two days of autonomy, the cost of battery is significant and contributes to 43% of the total cost. Besides, the hydrogen produced is mainly stored as compressed gas and transported via gas trailers and pipelines. When the days of autonomy is increased to 8 and above, electricity storage and transportation in the form of hydrogen is preferred, and the transported hydrogen is reconverted back to electricity at demand regions through fuel cells. On the other hand, for hydrogen demands at refueling stations, hydrogen produced from electrolyzer is stored and transported to refueling stations in the form of LOHC.

From the sensitivity analysis, it is shown that HESC is unlikely to fully replace the conventional energy system in

near-future due to the high cost of investment. For further studies, the HESC optimization framework can be further extended to include multi-period modeling to model the stagewise development of hydrogen supply network in order to fulfil the fuel and electricity penetration targets for each time period. Moreover, environmental and safety indexes should be incorporated into the proposed framework for multi-objective optimization of HESC.

Supplementary Information The online version contains supplementary material available at https://doi.org/10.1007/s10098-021-02235-4.

Acknowledgements The authors would like to thank Universiti Teknologi Malaysia (UTM) for financial support under the grants Q.J130000.3051.02M03, Q.J130000.2851.00L51, and Q.J130000.3551.06G47. This research is also supported by a grant from the National Research Foundation, Prime Minister Office, Singapore under its Energy and Environmental Sustainability for Megacities (E2S2), Campus of Research Excellence and Technological Enterprise (CREATE) programme.

Authors' contributions Conceptualization was done by Angel Xin Yee Mah, Wai Shin Ho, Gabriel Hoh Teck Ling, and Chin Siong Ho; methodology was done by Angel Xin Yee Mah; writing—original draft preparation was done by Angel Xin Yee Mah; writing—reviewing and editing was done by Angel Xin Yee Mah and Wai Shin Ho; supervision was done by Wai Shin Ho, Mimi H. Hassim, and Haslenda Hashim; resources were gathered by Mimi H. Hassim and Haslenda Hashim; validation was done by Zarina Ab Muis, Gabriel Hoh Teck Ling, and Chin Siong Ho.

Funding The authors would like to thank Universiti Teknologi Malaysia (UTM) for financial support under the grants Q.J130000.3051.02M03, Q.J130000.2851.00L51, and Q.J130000.3551.06G47. This research is also supported by a grant from the National Research Foundation, Prime Minister Office, Singapore under its Energy and Environmental Sustainability for Megacities (E2S2), Campus of Research Excellence and Technological Enterprise (CREATE) programme.

Data availability The authors declare that data supporting the findings of this study are available within the article and its supplementary information files.

Declarations

Conflict of interest Not applicable.

References

Acar C, Dincer I (2018) 1.13 Hydrogen Energy. In: Dincer I (ed) Comprehensive energy systems. Elsevier, pp 568–605

Almaraz SD-L, Azzaro-Pantel C, Montastruc L, Boix M (2015) Deployment of a hydrogen supply chain by multi-objective/multi-period optimisation at regional and national scales. Chem Eng Res Des 104:11–31. https://doi.org/10.1016/j.cherd.2015.07.005

Cho S, Kim J (2019) Multi-site and multi-period optimization model for strategic planning of a renewable hydrogen energy network from biomass waste and energy crops. Energy 185:527–540

Dagdougui H (2012) Models, methods and approaches for the planning and design of the future hydrogen supply chain. Int J Hydrogen Energy 37(6):5318–5327. https://doi.org/10.1016/j.ijhydene.2011.08.041

DIVA-GIS (2021) Download data by country. https://www.diva-gis.org/gdata. Accessed 14 April 2021

Energy Commission (2019) Malaysia Energy Statistics Handbook 2018. https://meih.st.gov.my/documents/10620/c7e69704-6f80-40ae-a764-ad0acf4a844d. Accessed 16 October 2021

H2 Mobility (2021) Toyota MIRAI. https://h2.live/en/wasserstoffautos/toyota-mirai-ii. Accessed 7 April 2021

Huang Z, Xie Z, Zhang C, Chan SH, Milewski J, Xie Y, Yang Y, Hu X (2019) Modeling and multi-objective optimization of a standalone PV-hydrogen-retired EV battery hybrid energy system. Energy Convers Manage 181:80–92

Hydrogen Council (2017) How hydrogen empowers the energy transition. https://hydrogencouncil.com/wp-content/uploads/2017/06/Hydrogen-Council-Vision-Document.pdf. Accessed 16 October 2021

IEA (2019) The Future of Hydrogen. Paris, https://www.iea.org/reports/the-future-of-hydrogen. Accessed 15 April 2021

IEA (2020) Batteries and hydrogen technology: keys for a clean energy future. Paris, https://www.iea.org/articles/batteries-and-hydrogen-technology-keys-for-a-clean-energy-future. Accessed 15 April 2021

Johnson N, Ogden J (2012) A spatially-explicit optimization model for long-term hydrogen pipeline planning. Int J Hydrogen Energy 37(6):5421–5433. https://doi.org/10.1016/j.ijhydene.2011.08.109

Kim M, Kim J (2016) Optimization model for the design and analysis of an integrated renewable hydrogen supply (IRHS) system: application to Korea's hydrogen economy. Int J Hydrogen Energy 41:16613–16626. https://doi.org/10.1016/j.ijhydene.2016.07.079

Li L, Manier H, Manier M-A (2019) Hydrogen supply chain network design: an optimization-oriented review. Renew Sustain Energy Rev 103:342–360. https://doi.org/10.1016/j.rser.2018.12.060

Li L, Manier H, Manier M-A (2020) Integrated optimization model for hydrogen supply chain network design and hydrogen fueling station planning. Comput Chem Eng 134:106683

MaCGDI (2010) Malaysian Centre for Geospatial Data Infrastructure. http://www.mygeoportal.gov.my/. Accessed 26 October 2017

Martin A, Agnoletti M-F, Brangier E (2020) Users in the design of hydrogen energy systems: a systematic review. Int J Hydrogen Energy. https://doi.org/10.1016/j.ijhydene.2020.02.163

Maryam S (2017) Review of modelling approaches used in the HSC context for the UK. Int J Hydrogen Energy 42(39):24927–24938. https://doi.org/10.1016/j.ijhydene.2017.04.303

Moreno-Benito M, Agnolucci P, Papageorgiou LG (2017) Towards a sustainable hydrogen economy: optimisation-based framework for hydrogen infrastructure development. Comput Chem Eng 102:110–127. https://doi.org/10.1016/j.compchemeng.2016.08.005

Ochoa Bique A, Zondervan E (2018) An outlook towards hydrogen supply chain networks in 2050 — design of novel fuel infrastructures in Germany. Chem Eng Res Des 134:90–103. https://doi.org/10.1016/j.cherd.2018.03.037

Ogumerem GS, Kim C, Kesisoglou I, Diangelakis NA, Pistikopoulos EN (2018) A multi-objective optimization for the design and operation of a hydrogen network for transportation fuel. Chem Eng Res Des 131:279–292. https://doi.org/10.1016/j.cherd.2017.12.032

Reuß M, Grube T, Robinius M, Preuster P, Wasserscheid P, Stolten D (2017) Seasonal storage and alternative carriers: a flexible hydrogen supply chain model. Appl Energy 200:290–302

Reuß M, Grube T, Robinius M, Stolten D (2019) A hydrogen supply chain with spatial resolution: comparative analysis of infrastructure technologies in Germany. Appl Energy 247:438–453. https://doi.org/10.1016/j.apenergy.2019.04.064

Robles JO, Azzaro-Pantel C, Aguilar-Lasserre A (2020) Optimization of a hydrogen supply chain network design under demand uncertainty by multi-objective genetic algorithms. Comput Chem Eng 140:106853

Samsatli S, Samsatli NJ (2019) The role of renewable hydrogen and inter-seasonal storage in decarbonising heat – comprehensive optimisation of future renewable energy value chains. Appl Energy 233–234:854–893. https://doi.org/10.1016/j.apenergy.2018.09.159

Samsatli S, Staffell I, Samsatli NJ (2016) Optimal design and operation of integrated wind-hydrogen-electricity networks for decarbonising the domestic transport sector in Great Britain. Int J Hydrogen Energy 41(1):447–475. https://doi.org/10.1016/j.ijhydene.2015.10.032

Seo S-K, Yun D-Y, Lee C-J (2020) Design and optimization of a hydrogen supply chain using a centralized storage model. Appl Energy 262:114452

Shabadin A, MegatJohari N, Mohamed Jamil H (2014) Car annual vehicle kilometer travelled estimated from car manufacturer data–an improved method. Pertanika 25(1):171–180

Shamsi H, Tran M-K, Akbarpour S, Maroufmashat A, Fowler M (2021) Macro-level optimization of hydrogen infrastructure and supply chain for zero-emission vehicles on a Canadian corridor. J Clean Prod 289:125163

Solargis (2020) Solar resource maps of Malaysia. https://solargis.com/maps-and-gis-data/download/malaysia. Accessed 5 Jan 2020

USGS (2015) USGS EROS Archive - Digital elevation - shuttle radar topography mission (SRTM) 1 Arc-Second Global. https://www.usgs.gov/centers/eros/science/usgs-eros-archive-digital-elevation-shuttle-radar-topography-mission-srtm-1-arc?qt-science_center_objects=0#qt-science_center_objects. Accessed

Welder L, Ryberg DS, Kotzur L, Grube T, Robinius M, Stolten D (2018) Spatio-temporal optimization of a future energy system for power-to-hydrogen applications in Germany. Energy 158:1130–1149. https://doi.org/10.1016/j.energy.2018.05.059

Welder L, Stenzel P, Ebersbach N, Markewitz P, Robinius M, Emonts B, Stolten D (2019) Design and evaluation of hydrogen electricity reconversion pathways in national energy systems using spatially and temporally resolved energy system optimization. Int J Hydrogen Energy 44(19):9594–9607. https://doi.org/10.1016/j.ijhydene.2018.11.194

Won W, Kwon H, Han JH, Kim J (2017) Design and operation of renewable energy sources based hydrogen supply system: technology integration and optimization. Renew Energy 103:226–238. https://doi.org/10.1016/j.renene.2016.11.038

Woo YB, Cho S, Kim J, Kim BS (2016) Optimization-based approach for strategic design and operation of a biomass-to-hydrogen supply chain. Int J Hydrogen Energy 41:5405–5418. https://doi.org/10.1016/j.ijhydene.2016.01.153

WorldPop (2018) Population Counts. https://www.worldpop.org/geodata/listing?id=29. Accessed 15 April 2021